Supporting Information

Heifets *et al.* 10.1073/pnas.0711880105

SI Results

Do Test Pulses Contribute to I-LTD Induction? I-LTD does not require continuously evoked test stimuli (.067 Hz) during the induction period, in contrast to presynaptic LTD at excitatory synapses (TBS, stop stimulation, 18.8 ± 2.6%, $n = 6$ vs. TBS, 21.6 ± 2.7%, $n = 10$; $P = 0.51$) [supporting information (SI) Fig. S1*A*] (1–3).

CB1R-Containing Inputs Significantly Contribute to Basal Inhibitory Spontaneous Activity. One of the hallmark differences between inhibitory and excitatory synapses is the degree of basal spontaneous activity. Indeed, GABAergic interneurons of the hippocampus show a high degree of spontaneous activity both *in vivo* and *in vitro* (4, 5). If CB1R containing interneurons must be active to support I-LTD, baseline recording conditions in our slices should include a measurable proportion of sIPSCs sensitive to the CB1R agonist WIN55,212–2 (WIN; 5 μM). Presynaptic CB1Rs inhibit GABA release, and consistent with this mechanism, WIN significantly suppressed the frequency, rather than the amplitude of sIPSCs, in agreement with a previous study (control, 13.1 ± 1.9 Hz, $n = 5$, vs. 5 μM WIN, 9.2 ± 1.4 Hz, $n = 5$; $P < 0.01$; control, 25.0 ± 3.4 pA vs. 21.0 ± 2.3 pA; $P = 0.11$) (Fig. S1*B Upper* and Fig. S1*B Lower*, respectively) (6).

A Low Dose of TTX Significantly Blocks IN Firing and sIPSCs While Preserving evIPSCs. To assess the contribution of sIPSCs to I-LTD induction, we used a low dose of TTX (10 nM) to suppress spontaneous interneuron firing. In a single hippocampal slice, we simultaneously recorded spontaneous firing of one interneuron (see *SI Methods*) and monitored IPSCs from a nearby CA1 PC, evoked with an extracellularly placed stimulating pipette (Fig. S2*A*). Washing in 10 nM TTX selectively reduced the IN's firing without affecting the amplitude of evIPSCs. Ten nM TTX reduced firing of every interneuron tested (92.8 ± 1.8% reduction in frequency, $n = 4$) (Fig. S2*B*). Similarly, 10 nM TTX reduced the aggregate interneuron activity represented by sIPSCs. Under normal recording conditions, we observed frequent, large amplitude sIPSCs (Fig. S2*C*). Comparing 10 min and 20 min after adding 10 nM TTX, the initial sIPSC frequency of 9.2 ± 1.4 Hz fell to 5.7 ± 0.8 Hz ($n = 9$, $P < 0.01$). A high dose of TTX (500 nM), typically used to study miniature release events, further reduced sIPSC frequency to 4.3 ± 0.6 Hz ($n = 9$, $P < 0.01$ vs. 10 nM TTX). Both low and high doses of TTX shifted the distribution of sIPSCs toward lower amplitudes (10 nM and 500 nM TTX vs. No TTX, $P < 0.001$ and $P < 0.001$, respectively, K-S test) (Fig. S2*D*). Nonetheless, we could still evoke IPSCs by extracellular stimulation in the low dose of TTX (87.3 ± 1.5% of no TTX amplitude, $n = 5$) (Fig. S2*E*), but not in the high dose (0.1 ± 0.1% of no TTX amplitude, $n = 6$). A likely explanation for these observations is that partial blockade of sodium channels by a low dose of TTX increases the threshold for action potential generation. As a result, spontaneous firing rate of GABAergic interneurons is expected to be reduced. In contrast, extracellular stimulation used for evoking IPCS can be strong enough to depolarize the membrane and generate action potentials (provided Na channels are not fully blocked). In addition, spontaneous action potentials generated near the soma must travel a tortuous axon covered with branching points. Given that our extracellular stimulations of GABAergic axons are performed close to the recorded pyramidal cell, conduction failure may also contribute to the reduction of sIPCSs in 10 nM TTX.

IN Anatomical Identification in Cell Pair Recordings. The depicted IN from Fig. S3*A* was identified as a Schaffer-collateral-associated interneuron (7, 8). Two additional INs in this experimental group were reconstructed and identified as basket cells (9). The depicted interneuron from Fig. S3*B* was identified as a basket cell and another in the same group as a Schaffer-collateral-associated interneuron.

Cell Pairs and Functional Characterization. First, in terms of sIPSC frequency (recorded from the PC), all three groups of IN PC recordings (Fig. 2*D*) shared similar starting points, as well as DHPG-induced increases, indicating comparable levels of mGluR-I-induced activity and presumably eCB release across groups (pre-DHPG, DSI+, firing, 9.3 ± 1.6 Hz, DSI+, silent, 11.5 ± 3.3 Hz, DSI−, firing, 11.0 ± 3.2 Hz, n.s.d; during DHPG, DSI+, firing, 22.0 ± 3.3 Hz; DSI+, silent, 22.9 ± 3.2 Hz; DSI−, firing, 17.5 ± 3.2 Hz; n.s.d., one-way ANOVA) (Fig. S4*A*). Second, current injection into interneurons of DSI+, firing and DSI−, firing groups was adjusted to yield firing frequencies in the range observed during *in vivo* recordings (DSI+, firing, 2.4 ± 0.4 Hz; DSI+, silent, 0.0 ± 0.0 Hz; DSI−, firing, 2.8 ± 0.4 Hz; DSI+, firing vs. DSI−, firing; $P = 0.32$) (Fig. S4*B*) (10, 11). The comparable firing rates render it unlikely that presynaptic firing alone accounts for the magnitude of I-LTD. Third, LTD in cell pairs (Fig. 2*D*) and TBS-induced I-LTD are expressed in an identical fashion. Significant increases in two measures of neurotransmitter release probability, transmission failure rate (FR) and paired pulse ratio (PPR), indicate that the observed long-term depression has a presynaptic site of expression, like TBS induced I-LTD (FR, DSI+, firing: pre, 0.07 ± 0.03 vs. post, 0.42 ± 8.2; $P < 0.01$; PPR, DSI+, firing: pre, 0.73 ± 0.11 vs. post, 1.31 ± 0.21; $P < 0.05$) (Fig. S4*C*) (12). When INs were held silent during DHPG, these parameters did not change FR, DSI+, silent: pre, 0.12 ± 0.07 vs. post, 0.09 ± 0.07; $P = 0.1$; PPR, DSI+, silent: pre, 0.87 ± 0.07 vs. post, 0.88 ± 0.04; $P = 0.83$) (Fig. S4*D*). It is also worth noting that the DSI+ groups had comparable starting points by these measures (FR, pre: DSI+, silent vs. DSI+, firing; $P = 0.47$; PPR, pre: DSI+, silent vs. DSI+, firing; $P = 0.34$) (Fig. S4*C* and Fig. S4*D*, respectively).

Postsynaptic Ca^{2+} Is Not Required for I-LTD. Buffering postsynaptic Ca^{2+} does not change the magnitude of I-LTD (control, 21.6 ± 1.4%, $n = 5$ vs. BAPTA post, 19.7 ± 2.0%, $n = 7$; $P = 0.50$) (Fig. S5*A*), which allows us to target presynaptic calcium homeostasis through manipulations of the perfused bath solution.

Block of I-LTD by EGTA-AM Is Not Due to Reduced IN Firing. We monitored spontaneous IN firing with extracellular recordings under the same conditions used to measure I-LTD; 100 μM EGTA-AM had no effect on the spontaneous firing of individual interneurons, although over the same time period (separate experiments), EGTA-AM had depressed evIPSCs to a steady state (Spikes, pre, 2.7 ± 0.6 Hz vs. post, 2.4 ± 0.5 Hz, $n = 6$; $P = 0.53$; IPSCs, 56.3 ± 9.8% depression, $n = 2$) (Fig. S5*B*).

Changes in Spontaneous Activity Do Not Account for the Block of I-LTD by CPA or Thapsigargin. The SERCA blockers (used in Fig. 3*C*) did not significantly change the average sIPSC frequency or amplitude distribution in the period following the TBS (Frequency: control, 18.1 ± 3.0 Hz vs. CPA/TG, 17.1 ± 3.8 Hz; $P = 0.85$; Amplitude: control, 28.8 ± 1.6 pA vs. CPA/TG, 28.9 ± 3.9 pA;

$P = 0.97$) (Fig. S5*C*), arguing against a simple reduction of IN activity as the mechanism of I-LTD blockade

Disruption of CB1R Function Does Not Account for the Block I-LTD by SERCA Blockers, EGTA-AM, or Protein Phosphatase Inhibitors. Figs. 3 and 4 show that I-LTD is blocked by several bath-applied compounds. The loss of I-LTD could have simply been due to a reduction in the number or efficacy of CB1Rs in hippocampal slices treated with these drugs. We compared the acute depression of fIPSPs by the CB1R agonist WIN in naive slices (control) to two groups of slices treated with different drug cocktails, corresponding to the drugs used in Figs. 3 and 4, respectively. In each case, drugs were applied in the same dose and duration as used to block I-LTD. One group (CPA, TG, and EGTA-AM) was incubated in CPA (30 μM) and TG (2 μM) for 30–60 min before the recording, and pretreated for 30 min with EGTA-AM (100 μM); experiments with these slices were performed in the continuous presence of CPA and TG, but not EGTA-AM. The second experimental group of slices (phosphatase inhibitors) was preincubated for 1–2 h with FK506 (50 μM), CyA (25 μM), and OKD (1 μM), and experiments were performed in the continuous presence of these drugs. WIN suppressed fIPSP to a similar extent in all three groups of slices, indicating that these drugs do not disrupt CB1R function (control, 27.3 ± 4.3%, n = 5; CPA, TG & EGTA-AM, 24.6 ± 5.6%, n = 4; PPIs, 27.6 ± 6.3%, n = 5; control vs. CPA, TG & EGTA-AM vs. phosphatase inhibitors, F <0.001; $P > 0.99$, one way ANOVA) (Fig. S6).

Presynaptic Calcineurin Is Required for I-LTD. We found that I-LTD depends on CaN, but not on PP1/2A (Fig. 4 *A* and *C*). We were able to localize CaN′s relevant activity for I-LTD by loading the postsynaptic pipette with FK506 and testing I-LTD (Fig. 4*A*). Because neither postsynaptic FK506 nor bath applied OKD blocked I-LTD, we tested these compounds in another form of plasticity known to be sensitive to these compounds: LTD of AMPA receptors in CA1 pyramidal cells (E-LTD) (13). OKD was tested using field recordings (fEPSP). E-LTD of fEPSPs was successfully induced by delivering 600 pulses at 1 Hz in *s. radiatum* of CA1, performed in the presence of 50 μM picrotoxin (PTX). OKD fully blocked this E-LTD (control, 85.1 ± 2.1%, n = 13, vs. OKD, 107.0 ± 6.6%, n = 7; $P < 0.001$) (Fig. S7*B*). To test the efficacy of postsynaptic FK506, E-LTD was recorded in whole-cell configuration, voltage-clamp mode, with a holding potential between −70 and −65 mV. E-LTD was induced with 900 pulses at 5 Hz, during which time the pyramidal cell was depolarized to -40 mV. These experiments were also performed in the presence of PTX (50 μM). Once again, while robust E-LTD was observed under control conditions, loading postsynaptic cells with FK506 via the recording pipette blocked E-LTD, verifying FK506's efficacy (control, 58.2 ± 6.5%, n = 7, vs. FK post, 85.8 ± 9.4%, n = 7; $P < 0.05$) (Fig. S7*B*). In addition, we verified that CaN inhibitors were not blocking I-LTD by interfering with eCB/CB1R functioning. Bath applied CaN inhibitors (FK506, n = 4; CyA, n = 3) had no effect on DSI (control, 44.5 ± 11.4%, n = 6 vs. CaN inhibitors [data pooled for both compounds], 37.7 ± 5.3%, n = 7; $P = 0.58$), in accord with previously reported results (14).

Calcineurin Is Functional at GABAergic Terminals in CA1. As shown in Fig. 4*D*, blockade of CaN with FK506 enhanced the frequency, but not the amplitude, of mIPSCs recorded in CA1 pyramidal cells. Control recordings, where only the solvent was applied (0.05% ethanol), were stable for both frequency and amplitude over this period (Frequency, pre: 7.4 ± 1.9 Hz vs. post vehicle: 8.3 ± 2.4 Hz, n = 3; $P = 0.41$; Amplitude, pre: 14.2 ± 1.0 pA vs. post vehicle: 13.1 ± 1.1 pA, n = 3; $P = 0.09$). Like FK506, CyA also produced a slow and significant enhancement of mIPSC frequency without affecting average mIPSC amplitude (Frequency: pre, 8.0 ± 1.9 Hz vs. Post CyA, 14.7 ± 1.5 Hz, n = 6; $P <$ 0.05; Amplitude: Pre, 17.5 ± 0.7 pA vs. post CyA, 20.2 ± 2.1 pA, n = 6; $P = 0.17$)

SI Methods

IN Spike Recordings. Cell bodies were visually identified in *s. radiatum* of CA1. Extracellular spike recordings were performed by placing recording pipettes filled with 1M NaCl at various sites near the interneuron soma. Action potential-generative zones near the soma were detected by stimulating firing with a brief (≈5 s) puff of extracellular recording solution containing 6.5 mM KCl over the slice. Once positioning of the recording pipette was optimized for spike detection, the experiments were performed in the same recording conditions as for whole-cell IPSCs. Spikes were detected with customized software for IgorPro.

Cell Pair Recordings. Simultaneous recordings were obtained from 308 INs and 481 PCs. Synaptic connections were evident in 195 cases (≈41%), with uIPSCs ranging from 15 - 2500 pA. For this study, cell pairs with failure rate >50% and uIPSC <100 pA were excluded. To test cell pairs for DSI, IN APs were evoked every 5 s; after ≈1 min of stable uIPSC amplitude, the PC was depolarized to 0 mV for 5 s. IN stimulation resumed after recovery of the PC holding current. DSI was tested at least three times per cell pair, and classified as DSI+ if at least two DSI attempts yielded an average suppression of >50% in the 20 s after depolarization. DSI was detected in 32 of 151 cell pairs. Multiple DSIs were averaged for each cell pair before cross-experiment averaging. The peak inhibition during DSI was quantified by averaging IPSC amplitudes 6 and 12 s after depolarization. For LTD measurement in cell pairs, IN APs were evoked every 10–15 s. In most cases, the $GABA_B$ antagonist CGP 55,845 was added to the extracellular recording solution. In two DSI+ cell pairs, DSI was blocked by perfusing a CB1R antagonist AM251 (5 μM), which also blocked subsequent I-LTD (DHPG plus IN firing). These cell pairs were included with the DSI−, firing group.

IN Labeling and Reconstruction. In some cell pair recordings, biocytin (0.2%) was included in the interneuron recording pipette, and slices were fixed at the experiments' end in 4% paraformaldehyde and 0.2% picric acid overnight at 4°C. In between washes with PBS, slices were treated with 1% H2O2 for 2.5 h to reduce endogenous peroxidase activity. Slices were cryoprotected in 30% sucrose for 2h, and then rapidly frozen using FreezeIt (Imeb). Slices were immediately replaced into 30% sucrose with 3% Triton X-100. Biocytin was detected by incubating sections overnight with an avidin–biotin–horseradish peroxidase complex (Elite ABC; Vector Laboratories). The horseradish peroxidase reaction was developed with 3,3′-diaminobenzidine tetrahydrochloride w/Co (D-0426; Sigma–Aldrich), and quenched with H_2O. Slices were dehydrated, cleared in xylene, and coverslipped with Permount (Fisher). Morphological reconstructions were made with camera lucida at 25× magnification.

Miniature IPSCs. mIPSC recordings were performed with the same internal solution used for sIPSCs and evIPSCs, and membrane potential was clamped at +20 mV. The ACSF solution contained 500 nM TTX, 100 μM $CdCl_2$, 5 mM $CaCl_2$, 25 μM d-APV, and 10 μM NBQX, and experiments were performed at 28.0 ± 0.1°C.

Chemicals. Unless otherwise stated, drugs were bath applied after dilution into the ACSF from concentrated stock solutions. SR141716 (NIMH), NBQX (Tocris or Ascent), EGTA-AM (Anaspec), CPA, TG, CGP 55845, AM251, and WIN 55,212–2 (Tocris) were dissolved in DMSO. FK506 (LC Labs) was dis-

solved in EtOH (final concentration in ACSF: 0.1% EtOH). CyA (Tocris) was dissolved in a 2:1 EtOH:Tween80 (final concentration in ACSF: 0.1% ethanol and 0.05% Tween 80). Okadaic acid (potassium salt; LC Labs or Calbiochem), TTX (Sigma), d-APV (Tocris or Ascent), DHPG, and MPEP (Tocris) were dissolved in water, and LY367385 (Tocris) was dissolved in water and 1 eq NaOH. For experiments involving drug treatment of slices, interleaved controls were performed in the same concentration of respective solvent. All drugs were stored as stock solutions at −20°C before use.

1. Tzounopoulos T, Janz R, Sudhof TC, Nicoll RA, Malenka RC (1998) A role for cAMP in long-term depression at hippocampal mossy fiber synapses. *Neuron* 21:837–845.
2. Sjostrom PJ, Turrigiano GG, Nelson SB (2003) Neocortical LTD via coincident activation of presynaptic NMDA and cannabinoid receptors. *Neuron* 39:641–654.
3. Singla S, Kreitzer AC, Malenka RC (2007) Mechanisms for synapse specificity during striatal long-term depression. *J Neurosci* 27:5260–5264.
4. Somogyi P, Klausberger T (2005) Defined types of cortical interneurone structure space and spike timing in the hippocampus. *J Physiol* 562:9–26.
5. Fricker D, Verheugen JA, Miles R (1999) Cell-attached measurements of the firing threshold of rat hippocampal neurons. *J Physiol* 517(Pt 3):791–804.
6. Hoffman AF, Lupica CR (2000) Mechanisms of cannabinoid inhibition of GABA(A) synaptic transmission in the hippocampus. *J Neurosci* 20:2470–2479.
7. Cope DW, *et al*. (2002) Cholecystokinin-immunopositive basket and Schaffer collateral-associated interneurones target different domains of pyramidal cells in the CA1 area of the rat hippocampus. *Neuroscience* 109:63–80.
8. Pawelzik H, Hughes DI, Thomson AM (2002) Physiological and morphological diversity of immunocytochemically defined parvalbumin- and cholecystokinin-positive interneurones in CA1 of the adult rat hippocampus. *J Comp Neurol* 443:346–367.
9. Freund TF, Buzsaki G (1996) Interneurons of the hippocampus. *Hippocampus* 6:347–470.
10. Klausberger T, et al. (2003) Brain-state- and cell-type-specific firing of hippocampal interneurons *in vivo*. *Nature* 421:844–848.
11. Klausberger T, *et al*. (2005) Complementary roles of cholecystokinin- and parvalbumin-expressing GABAergic neurons in hippocampal network oscillations. *J Neurosci* 25:9782–9793.
12. Chevaleyre V, Castillo PE (2003) Heterosynaptic LTD of hippocampal GABAergic synapses: A novel role of endocannabinoids in regulating excitability. *Neuron* 38:461–472.
13. Malenka RC, Bear MF (2004) LTP and LTD: An embarrassment of riches. *Neuron* 44:5–21.
14. Wilson RI, Kunos G, Nicoll RA (2001) Presynaptic specificity of endocannabinoid signaling in the hippocampus. *Neuron* 31:453–462.
15. Wang J, *et al*. (2003) Interaction of calcineurin and type-A GABA receptor gamma 2 subunits produces long-term depression at CA1 inhibitory synapses. *J Neurosci* 23:826–836.
16. Jones MV, Westbrook GL (1997) Shaping of IPSCs by endogenous calcineurin activity. *J Neurosci* 17:7626–7633.
17. Sik A, Hajos N, Gulacsi A, Mody I, Freund TF (1998) The absence of a major Ca^{2+} signaling pathway in GABAergic neurons of the hippocampus. *Proc Natl Acad Sci USA* 95:3245–3250.

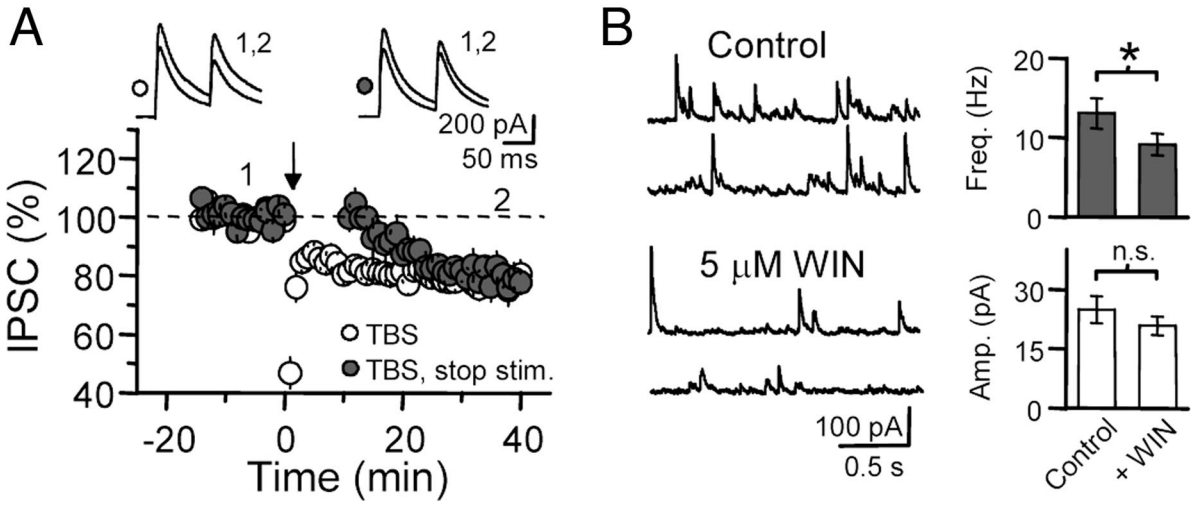

Fig. S1. (*A*) Unlike other forms of eCB-LTD, I-LTD induction does not depend on evoked synaptic stimulation during the time period when CB1R activation is required. (*B*) Spontaneous activity is a prominent characteristic of inhibition in the hippocampus (*Upper Left*, traces). The CB1R agonist WIN 55,212 (5 μM) reveals the contribution of CB1R-sensitive afferents by inhibiting GABA release from those inputs. WIN significantly reduced sIPSC frequency, but not average sIPSC amplitude.

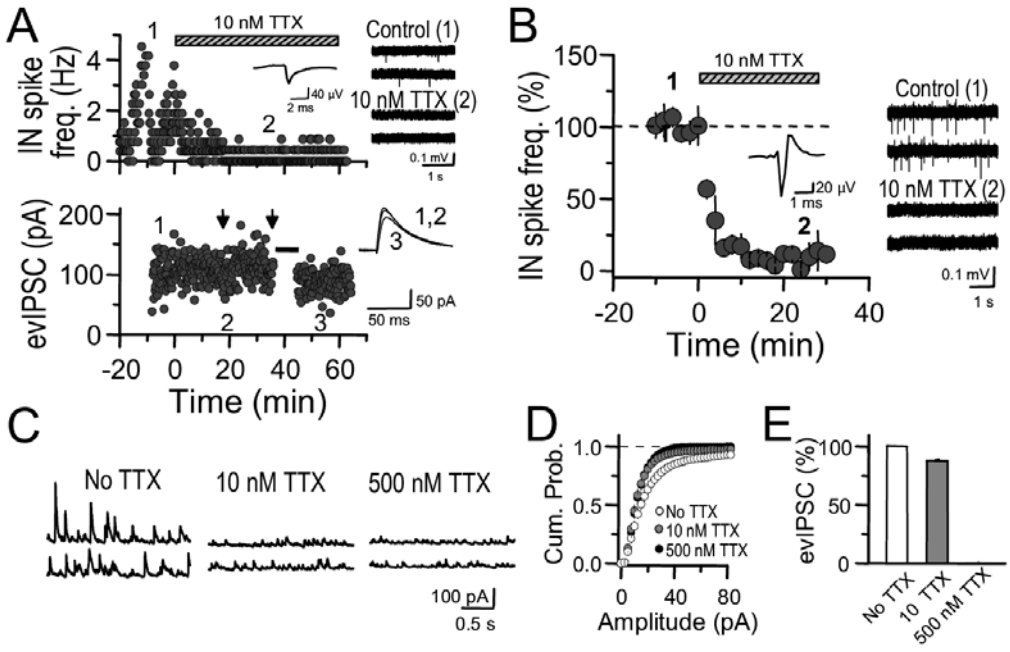

Fig. S2. A low dose of tetrodotoxin reduces spontaneous interneuron firing while preserving evoked IPSCs. (*A*) A single experiment where an individual interneuron's firing is monitored by extracellular field recording (*Upper*) at the same time as whole-cell electrically evoked IPSCs (evIPSCs) are recorded from a CA1 pyramidal cell (*Lower*). Averaged spike waveform shown as inset, top. 10 nM TTX does not affect evIPSC amplitude, but it greatly reduces interneuron firing. In this experiment, I-LTD was also tested: 10 nM TTX blocked the first attempt at I-LTD induction, but I-LTD could be rescued by supplying extracellular stimulation after a subsequent TBS. Traces shown at indicated time points. (*B*) Summary of 10 nM TTX's effect on spontaneous interneuron firing. Traces from a different experiment than in A are shown at right for indicated time points. Averaged spike waveform shown as inset. (*C*) sIPSCs are a salient feature of cellular activity under normal recording conditions, whose frequency and average amplitude can be reduced by TTX. (*D*) A substantial proportion of these sIPSCs, especially large amplitude events, are action potential-driven: Both a low and high dose of TTX (center, right traces in *C*) significantly skewed the event distribution toward lower amplitudes. (*E*) In 10 nM TTX, IPSCs could still be evoked, but not in 500 nM TTX.

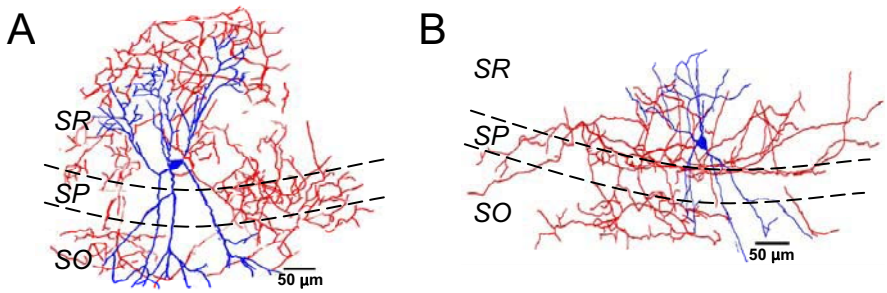

Fig. S3. Interneuron reconstructions for the experiments shown in Fig. 2 *A* and *B*.

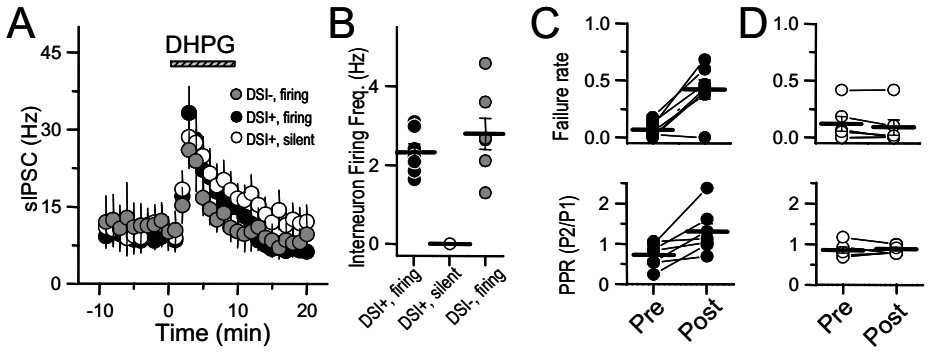

Fig. S4. Summary data for interneuron-pyramidal cell paired recordings. (*A*) Frequency of sIPSCs recorded from the pyramidal cell before and during DHPG application. Baseline sIPSC frequency was similar in all three groups, and increased to similar levels during DHPG application. (*B*) Average and distribution of interneuron firing rates during 10 min of DHPG application for each cell pair group. (*C* and *D*) Like I-LTD of evoked IPSCs, long-term depression in DSI+ cell pairs decreases the probability of neurotransmitter release. Initially (pre), both DSI+ groups have similar failure rates and paired pulse ratios. However, after DHPG (post), DSI+, firing cell pairs show a significantly enhanced FR (*C Upper*) and higher PPR (*C Lower*), whereas DSI+, silent cell pairs do not (*D Upper* and *Lower*).

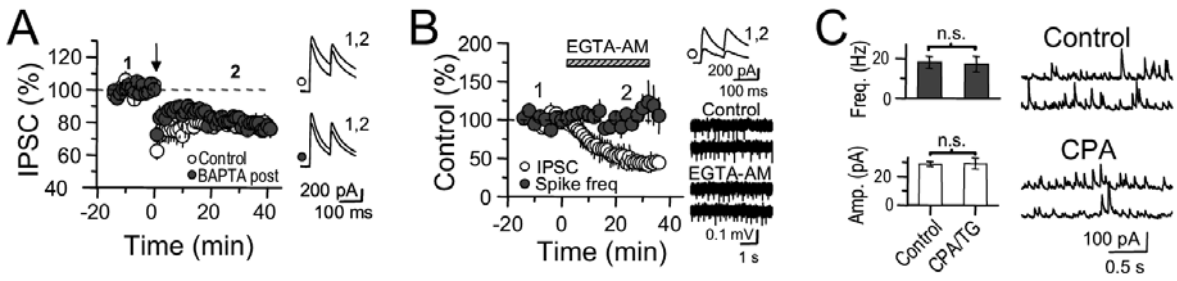

Fig. S5. Neither postsynaptic calcium nor changes of interneuron activity account for the block of I-LTD by bath manipulations of calcium homeostasis. (*A*) Postsynaptic BAPTA had no effect on the magnitude of I-LTD compared to no BAPTA. (*B*) Over the same time period when 100 μM EGTA-AM reaches a saturating effect, interneuron spikes detected extracellularly are not reduced. (*C*) Changes in spontaneous activity do not account for the block of I-LTD by CPA/TG, as neither sIPSC frequency nor amplitude is significantly changed.

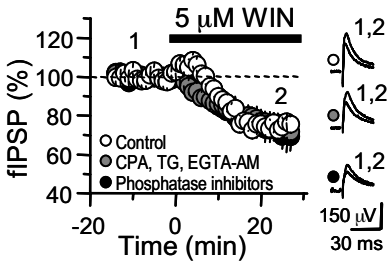

Fig. S6. WIN suppressed fIPSP to a similar extent when slices were treated with either of two cocktails of drugs, applied in the same dose and duration as in Figs. 3 and 4, respectively.

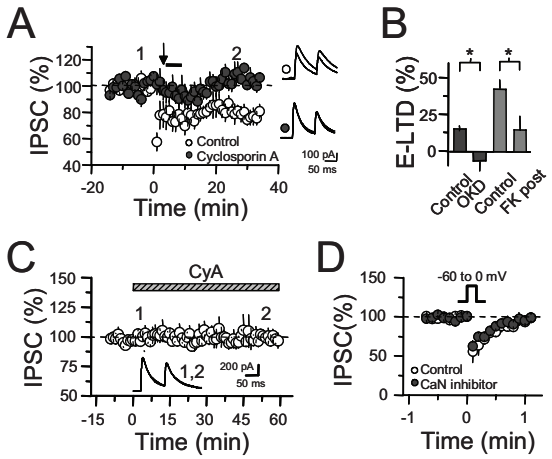

Fig. S7. (*A*) Like FK506, another blocker of CaN, CyA (25 μM) also blocked I-LTD induced by TBS and ''rescue'' activity. Solvent-alone controls (0.1% ethanol and 0.05% Tween 80) yielded normal I-LTD. (*B*) I-LTD was not affected by bath applications of a PP1/2A inhibitor, OKD, or by postsynaptically delivered FK506, yet both of these manipulations blocked LTD of AMPA receptors in CA1 pyramidal cells (E-LTD), indicating the efficacy of these drugs. (*C*) Blocking CaN with 25 μM CyA does not affect evoked IPSCs (n = 4). (*D*) CaN inhibitors (FK506, $n = 4$; CyA, $n = 3$) had no effect on DSI (induced by a 5-s step depolarization to 0 mV), indicating that these drugs do not impair eCB/CB1R signaling.